

# Effect of Microgravity on the Distribution of Liquid-Crystal Droplets Dispersed in a Polymer Matrix

K. Parbhakar, J. M. Jin, H. M. Nguyen, and L. H. Dao\*

*Laboratoire de recherche sur les matériaux avancés, INRS-Énergie et Matériaux, Institut National de la Recherche Scientifique, 1650 montée Ste-Julie, C.P. 1020, Varennes, Québec, Canada J3X 1S2*

Received October 16, 1995. Revised Manuscript Received March 7, 1996<sup>®</sup>

The average droplet size and their distribution in polymer-dispersed liquid-crystal (PDLC) materials, prepared under microgravity and terrestrial environments, are studied experimentally as a function of cure time. The PDLC films are prepared using a polymerization-induced phase-separation (PIPS) technique. A theoretical kinetic model, based on the birth-death type of differential equation, is developed. (This amounts to ignoring the coalescence produced by hydrodynamic motion.) Two important observations are reported in this study. The first, we found that microgravity plays a decisive role in establishing a Gaussian distribution of the liquid-crystal droplets which is in good agreement with theory. This behavior is maintained even if the droplets are allowed to grow substantially under terrestrial conditions provided the final stages of growth takes place under microgravity environment. The growth under microgravity conditions is diffusion dominated with an estimated effective spatial diffusion coefficient  $D = 3.78 \times 10^{-12} \text{ cm}^2 \text{ s}^{-1}$ , which seems appropriate for polymer matrix systems with high viscosities. The second result shows that the average particle size grows faster than the theoretically predicted  $t^{1/3}$  dependence. We believe that the coalescence processes that take place during the growth of droplets at 1 *g* during the cure time are responsible for this deviation.

## Introduction

Polymer-dispersed liquid-crystal (PDLC) materials have important industrial applications in information displays, optical shutters, and switchable windows.<sup>1,2</sup> A PDLC film is composed of micron-sized dispersion of liquid-crystal (LC) droplets within a polymer matrix. A simple way to prepare PDLC materials is to exploit the phase-separation phenomena. This can be accomplished (a) by cooling a thermoplastic/LC mixture below a critical solution temperature (thermal-induced phase separation or TIPS process), (b) through solvent evaporation of a solution-casted polymer/LC film (solvent-induced phase separation or SIPS process), or (c) by thermal or photopolymerization of the polymer precursor of the monomer/LC solution (polymerization-induced phase separation or PIPS process). The size and distribution of these droplets are the most important parameters that affect the electrooptical performance of PDLCs.<sup>3,4</sup> In the PIPS process, they are determined principally by composition, by cure rate and extent, and by mutual solubility of LC with the monomer. Usually, under terrestrial conditions, the phase separation (i.e., scaling properties) and the growth processes are greatly affected by sedimentation and convection.<sup>5</sup> Convection of droplets could be expected to affect coarsening

phenomena within films, in which the reduction of surface area drives the coalescence of droplets or domains. As shown recently,<sup>6</sup> the proximity of a surface can strongly influence the phase separation and also the subsequent domain growth of the phase. In this investigation we are mainly interested in the PIPS process and the surface tension driven growth is avoided by analyzing the data in regions far away from the surface and maintaining almost uniform temperature and concentration (Marangoni effects are not important). The presence of an ordering field such as gravity can also produce surface (capillary fluctuations) and network instabilities (sol-gel transformation) which can play an important role in the formation and growth processes.

In this study we introduce another film formation parameter, namely, the microgravity environment. In the case of PIPS process the phase transition is that of sol-gel type which is strongly influenced by gravity. In the SOL phase the polymer molecule clusters are relatively free to move and form networks which contain domains to be eventually filled with liquid crystal. Under 1 *g* the domains coalesce to produce distorted shapes which are then frozen on gelation. The driving force behind coalescence is the reduction in interfacial tension energy because of a small number of large surface domains. Furthermore the networks are not stable and may collapse under their own weight, producing spatial inhomogeneities. The final distribution is controlled by the competition between the polymerization reaction rate and the rate of reduction of free energy. However, in the case of microgravity environ-

<sup>®</sup> Abstract published in *Advance ACS Abstracts*, May 15, 1996.

(1) Doane, J. W.; Vaz, N. A.; Wu, B. G.; Zumer, S. *Appl. Phys. Lett.* **1986**, *48*, 269.

(2) Doane, J. W. *Liquid Crystal Applications and Uses*; Bahadur, B., Ed., World Scientific Publishers: River Edge, NJ, Vol. 1, Chapter 14.

(3) Parbhakar, K.; Dao, L. H.; Tabrizian, M.; Gingras, S.; Campbell, G. *Proc. Drop Tower Days 94*, July 8, 1994, Bremen, Germany; p 18.

(4) Alt, P. M.; Pleshko, P. *IEEE Trans. Electron Devices* **1974**, *21*, 146.

(5) Montgomery, Jr., G. P.; West, J. L.; Jamura-Lis, W. J. *J. Appl. Phys.* **1991**, *69*, 1605.

(6) Krausch, G.; Kramer, E. J.; Bates, F. S.; Marks, J. F.; Brown, G.; Chakrabarti, A. *Macromolecules* **1994**, *27*, 6768.

ment, diffusion is the major growth process producing spherical and more uniform domains. The interfacial tension is not affected by gravity. The final distribution here is controlled by the competition between the polymer reaction rate and the rate of reduction of the difference between the chemical potential of the inside and the outside regions of the domains. We present the effect of microgravity environment, as a function of time, on the spectrum of liquid-crystal droplets in a polymer matrix. Theory based on Smolouchowski type of equations which describe the growth of droplets under microgravity conditions is also developed. We find that when gravity is neglected, diffusion is the controlling process for growth and the droplet size distribution is Gaussian. This is in agreement with the experimental observation. The Gaussian distribution is obtained even if the specimen exposed to microgravity conditions for a short time in the final stages of the growth process.

### Experimental Section

The liquid crystal was a eutactic mixture designated as E7 (BDH Merck) which consists of 51% *n*-pentylcyanobiphenyl, 25% *n*-heptylcyanobiphenyl, 16% *n*-octylcyanobiphenyl, and 8% *n*-pentylcyanoterphenyl. The polymer matrix was a UV-curable resin NOA65 (Norland Products) which consists of trimethylpropanediallyl ether, trimethylolpropane trithiol, isophorone diisocyanate ester, and benzophenone photoinitiator.

The PDLC films were prepared by irradiation with a UV lamp ( $\lambda = 365$  nm and power = 100 mW/cm<sup>2</sup>) of predetermined mixtures of NOA65 and E7. A thin film (~5–20  $\mu$ ) of the mixture was spread between two glass substrates (transparent conductive electrode such as ITO glass). The film thickness was controlled by polycarbonate or polyimide film spacers.

Microgravity experiments were carried out at ZARM Drop Tower in Bremen Germany.<sup>7</sup> The PIPS apparatus consisted of a large-surface, high-power monochromatic UV lamp (Electro-Lite Co., Model ELC4000, 15 × 15 cm,  $\lambda = 365$  nm producing 100 mW/cm<sup>2</sup>) with an electrically activated mechanical shutter and a stabilized ac power supply, controllers, and probes for data acquisition during the drop experiment and a cell support. The cell support, which was made up of a thermoplastic insulator, could carry three sets of experiments. Each set consisted of three identical PDLC cells in order to ensure the reproducibility of our results. Variable lamp intensities were obtained by varying the distance of the cell support from the lamp. The drop capsule which hold the PIPS apparatus was sealed airtight and lifted to the top of the drop tower. The tower was evacuated and the capsule dropped for a 110 m free fall of 4.75 s at approximately 10<sup>-6</sup>g. A series of drops were carried out in order to determine the effect of microgravity and the role of other material processing parameters. In the case of the NOA65/E7 system, composition ratios of 40/60, 50/50, and 60/40 and fixed cure time of 4.75 s (drop experiments) and 3.3 s (after drop time) were used for each experiment. However, the irradiation time before the drop was varied from 2 to 6 s.

The morphology of the PDLC films was studied by scanning electron microscopy (SEM) using standard procedure. The cured samples was glued to an aluminum SEM stud and a section of the sample was removed from the top using a razor blade in order to achieve a flat surface (usually in the middle of the sample) for examination. The stud was placed in a sputtering unit evacuated to 10 mTorr of Hg for about an hour (this process removed practically all the liquid crystal from the exposed microdroplets). The sample was then coated with a thin Au-Pd coating to provide the conductive surface required for the SEM. The sample was then examined at

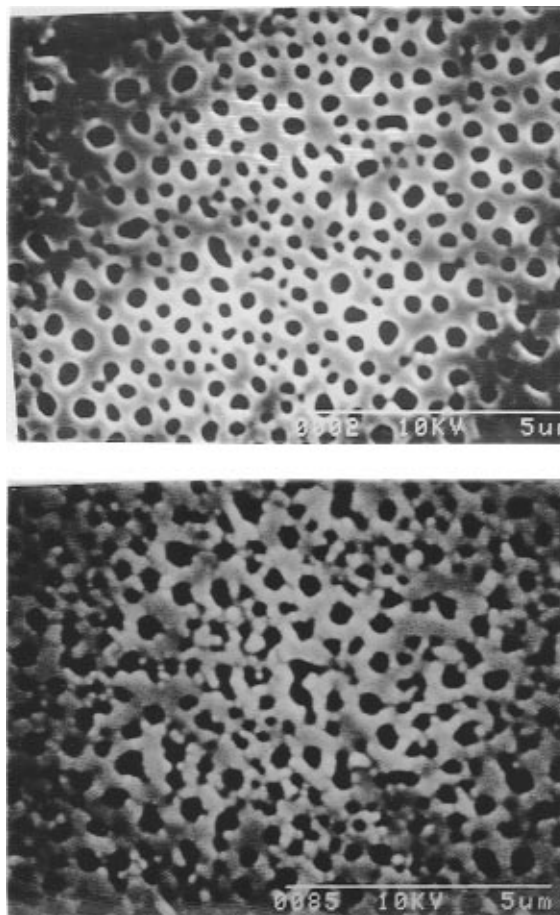


**Figure 1.** Scanning electron microscopy pictures for PIPS cells (NOA57/E7 50:50) at  $T = 25$  °C: (a, top) drop tower experiment (2 s at 1g, 4.75 s at 10<sup>-6</sup>g and 3.25 s at 1g) and (b, bottom) 10 s at 1g.

magnification up to 8000 $\times$ , using an acceleration potential of 15 kV. The solubility limit of liquid crystal in polymer matrix as well as fraction of liquid crystal which is dispersed as microdroplets were determined by differential scanning calorimetry (DSC).

### Results and Discussion

The typical morphology of PDLC films for a 50/50 NOA65/E7 blend is shown in Figures 1 and 2. Figure 1 shows the SEM pictures of two PDLC films prepared under similar conditions, except for gravity, irradiated for 10 s as followed: (a) 2.00 s before drop at 1g, 4.75 s at 10<sup>-6</sup>g, and 3.25 s at 1g after the drop, and (b) 10 s at 1g. Figure 2a shows the morphology of a PDLC film irradiated for 12 s (4.00 s at 1g, followed by 4.75 s at 10<sup>-6</sup>g, and 3.25 s at 1g) and Figure 2b for an identical PDLC film irradiated 12 s at 1g. From these pictures we note that under microgravity the liquid-crystal droplets (1) are nearly spherical in shape, (2) form less interconnected domains, and (3) are more uniformly dispersed.

Furthermore we note from these figures that the droplets are not uniform in size. From the analysis of the SEM pictures we can determine the size distribution. Figure 3 shows the droplet size distribution under terrestrial conditions for a cure time of 10 s, indicating a broad distribution. Figure 4 shows the size distribution under microgravity environment with the remaining parameters same as in Figure 3. An important

(7) Drop Tower-Bremen, User manual, version 2-1-2/91.

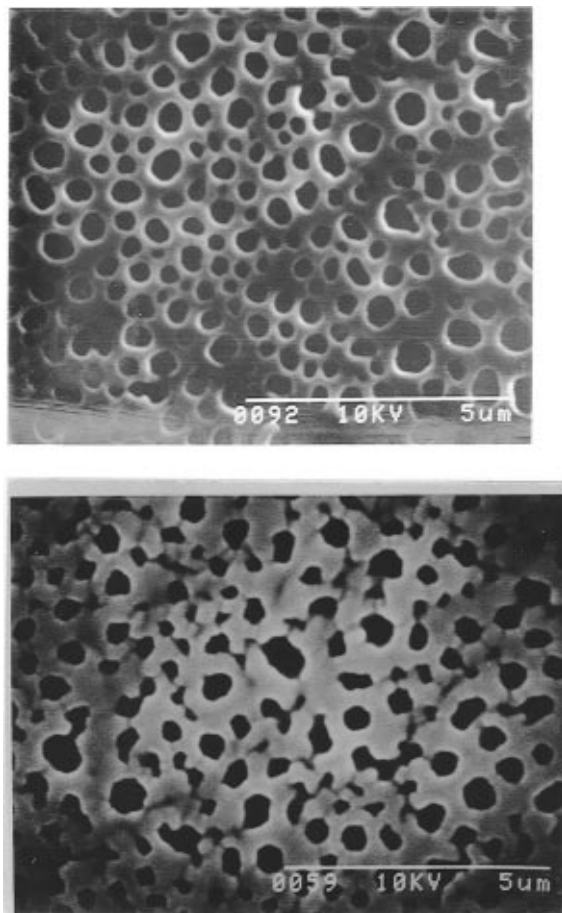


**Figure 2.** Scanning electron microscopy pictures for PIPS cells (NOA57/E7 50:50) at  $T = 25$  °C: (a, top) drop tower experiment (4 s at  $1g$ , 4.75 s at  $10^{-6}g$  and 3.25 at  $1g$ ) and (b, bottom) 12 s at  $1g$ .

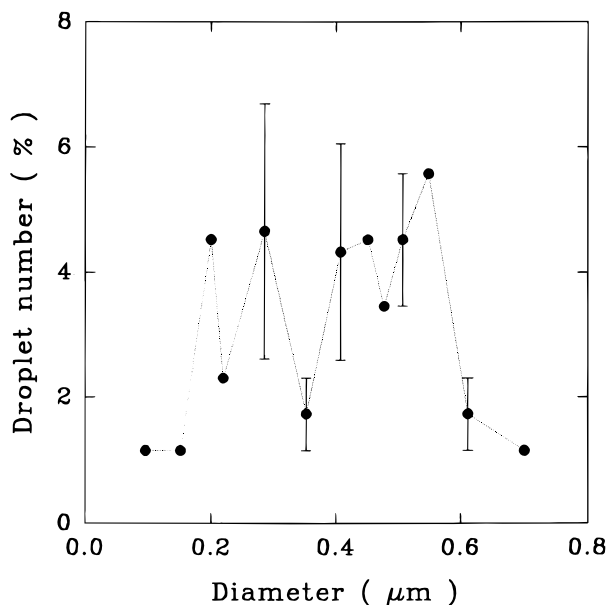


**Figure 3.** Droplet number (%) versus diameter at  $1g$  for a NOA57/E7 film (50:50 ratio) at  $T = 25$  °C and 12 s irradiation time.

distinction is observed between these two specimens. Under the microgravity environment the distribution is closer to a Gaussian distribution (a Gaussian fit is also shown in Figure 4; see theory below) as compared to the specimen prepared at  $1g$ . The average diameter in the two cases is approximately the same showing that

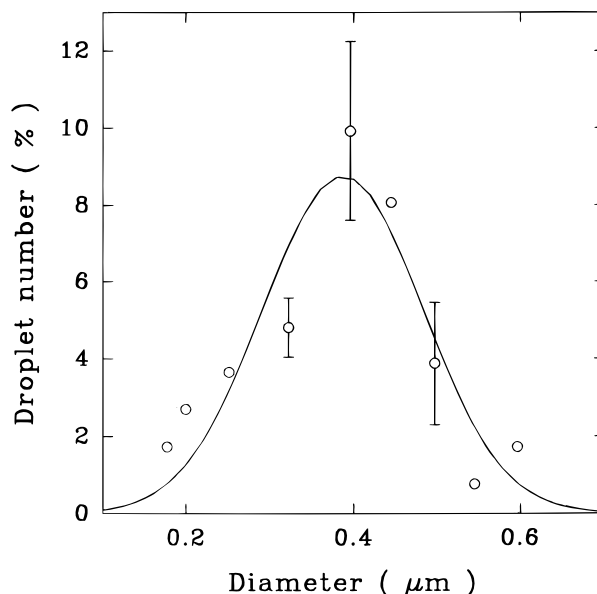


**Figure 4.** Droplet number (%) versus diameter at  $10^{-6}g$  for a NOA57/E7 film (50:50 ratio) at  $T = 25$  °C and 12 s irradiation time. The theoretical distribution is also shown where the best fit corresponds to  $D = 3.78 \times 10^{-12} \text{ cm}^2 \text{ s}^{-1}$ .

the average diameter is dependent only on the cure time which is held constant here.

To investigate the variation of average size with time and the changes produced in the distribution, the specimens were prepared for several cure times. Since the drop time is fixed, we varied the cure time before the drop between 2 and 6 s. In our system, as the polymerization starts the viscosity of the polymer matrix increases till a sol-gel type of phase transition takes place. Exact time of transition is difficult to determine under microgravity environment, but, however, scattering studies at  $1g$  in our laboratory and morphological investigation of UV-curable PDLC materials<sup>8</sup> indicate that the phase separation takes place between 2 and 5 s after the start of the polymerization process. Thus by varying the cure time between 2 and 6 s before the drop permits us to allow part of the growth to take place under terrestrial conditions (where coalescence may be predominant) and the remaining diffusive growth at  $10^{-6}g$ . This combined growth gives interesting results showing the effect of microgravity during the later stages of growth. The SEM pictures show that the size distribution approaches a Gaussian in all the three cases and the mean diameter increases nonlinearly with time. Figure 5 shows the variation of mean droplet diameter as a function of total cure time where the dispersion in the data is shown by vertical lines which represent the standard deviation  $2\sigma$  evaluated respectively from the Gaussian distributions at 10, 12, and 14 s. We find that in the case when the cure time is 14 s and the PDLC film spends a greater fraction of the preparation time at  $1g$ , the distribution is broader as compared to the 10 s cure time case, even if the distribution in both cases is Gaussian.

An interesting result is that even if the specimen is exposed to microgravity environment in the later stages of growth, the size distribution is Gaussian. In other

(8) Lovinger, S. J.; Amundson, K. R.; Davis, D. D. *Chem. Mater.* **1994**, *6*, 1726.

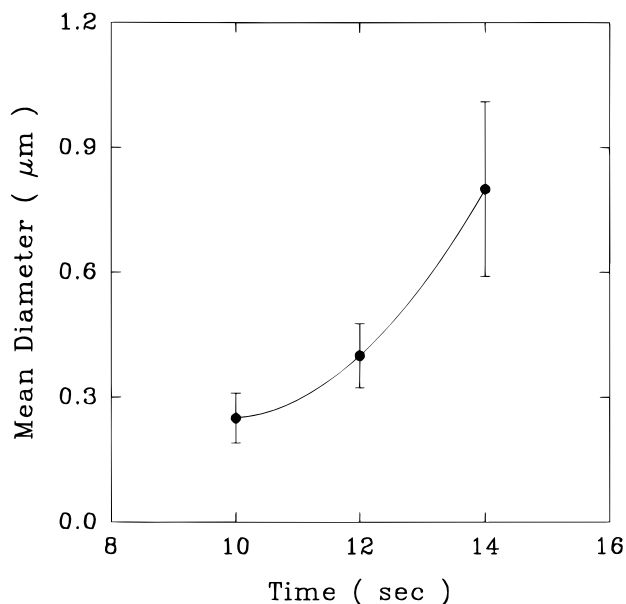


**Figure 5.** Mean diameter versus total irradiation time at  $10^{-6}g$ . The vertical bars show the dispersion ( $2\sigma$ ) for Gaussian distributions.

words, microgravity environment has a strong influence on the growth processes. As we show later in the following section that if the effects of a directed force such as gravity are neglected, the droplet distribution is expected to be Gaussian and the growth is diffusion dominated. We will also compute the average droplet size as a function of time. Experimentally we observed a much faster growth than predicted by theory, and we believe that this deviation is probably caused by coalescence produced during the cure process under terrestrial conditions (before the drop).

In the last section it was experimentally shown that the droplet size distribution in PDLC materials prepared under microgravity environment is Gaussian with a mean diameter which increases nonlinearly with cure time. We prove here that when the cluster aggregation or coalescence (produced either by convection or caused by hydrodynamic flows driven by interfacial tension) are neglected, the droplet distribution is Gaussian with a time-dependent mean radius. Neglecting the aggregation between droplets, considering the droplet as a cluster of molecules or particles, and assuming that the clusters change their size as a result of addition or loss of single particle, the rate of change of the population of clusters consisting of  $i$  particles,  $n_i$  is governed by eq 1<sup>9,10</sup> (the birth death process)

$$dn_i/dt = \beta_{i-1}n_{i-1} - \alpha_i n_i - \beta_i n_i + \alpha_{i+1}n_{i+1} = I_{i-1} - I_i \quad (1)$$

where  $\beta_i$  and  $\alpha_i$  are respectively the rate of condensation and evaporation of an  $i$ -population cluster and  $I_i$  denotes the net flux of clusters passing from  $i$  population to ( $i + 1$ ) population and is given by

$$I_i = \beta_i n_i - \alpha_{i+1} n_{i+1} \quad (2)$$

We have used the word particle in the sense that due to coarsening<sup>11</sup> (Ostwald ripening) processes the smallest size taking part in growth is given by the critical size. Furthermore the words cluster and droplet are synonymous to each other in this text, and we will use both without any confusion. Our model is more general than Ostwald ripening because in the later case the source for growth are small particles which must be continuously produced via condensation process and require supersaturation conditions. In our model the concentration of molecules is arbitrary. For a detailed description of Ostwald ripening we refer the reader to our recent publication.<sup>11</sup>

A strategy for dealing with the problem is the solution of the system of coupled difference equations with the intention of finding the size distribution and the mean droplet radius. It could only be undertaken numerically, of course, and as the aim is to understand the effect of gravitational field on droplet distribution, rather than to churn numerical results, we choose instead to make simplifying assumptions in the hope of obtaining analytical results. We first reduce the system of discrete equations to a single partial differential equation (Fokker-Planck equation). It is easy to show (see Appendix) that the system of equations 1 can be written as

$$\frac{\partial n(x,t)}{\partial t} = \frac{\partial}{\partial x} \left[ A(x) n(x,t) + \frac{\partial}{\partial x} (B(x) n(x,t)) \right] = - \frac{\partial}{\partial x} I(x,t) \quad (3)$$

where the discrete variable  $i$  is replaced by the continuous variable  $x$ , and

$$A(x) = \alpha(x) - \beta(x) \quad (4)$$

The net flux of clusters is now given by

$$B(x) = [\alpha(x) + \beta(x)]/2 \quad (5)$$

$$I = - A(x) n(x,t) - \frac{\partial}{\partial x} [B(x) n(x,t)] \quad (6)$$

Equation 3 is a partial differential equation with variable coefficients and is rather difficult to solve in its general form, particularly, because we have no knowledge regarding the variation of  $A$  and  $B$  with  $x$ . We will use the method of separation of variables to solve eq 3; however we, a priori, do not know if this equation is separable. We assume that eq 3 possesses a separable and a nonseparable solution, and we first determine the separable part of the solution. We propose

$$n(x,t) = N(x) \Phi(x,t) \quad (7)$$

where  $N(x)$  is the separable portion of the solution, and in what follows we will show that this corresponds to the equilibrium solution. Substituting eq 7 into eq 3,

(9) Nowakowski, B.; Ruckenstein, E. *J. Colloid Interface Sci.* **1991**, *145*, 182.

(10) Parbhakar, K.; Jin, J. M.; Dao, L. H. *J. Colloid Interface Sci.* **1995**, *174*, 414.

(11) Parbhakar, K.; Lewandowski, J.; Dao, L. H. *J. Colloid Interface Sci.* **1995**, *174*, 142.

we get

$$N(x) \frac{\partial \Phi(x,t)}{\partial t} = B(x) N(x) \frac{\partial^2 \Phi(x,t)}{\partial x^2} + 2 \frac{\partial \Phi(x,t)}{\partial x} \frac{\partial}{\partial x} [B(x) N(x)] + A(x) N(x) \frac{\partial \Phi(x,t)}{\partial x} + \Phi(x,t) \frac{\partial}{\partial x} \left[ A(x) N(x) + \frac{\partial}{\partial x} (B(x) N(x)) \right] \quad (8)$$

Now if we assume

$$A(x) N(x) + \frac{\partial}{\partial x} [B(x) N(x)] = 0 \quad (9)$$

Equation 8 reduces to

$$\frac{\partial \Phi(x,t)}{\partial t} = B(x) \frac{\partial^2 \Phi(x,t)}{\partial x^2} - A(x) \frac{\partial \Phi(x,t)}{\partial x} \quad (10)$$

Note that, physically, eq 9 corresponds to an equilibrium solution (detailed balancing) which represents a closed system (like ours); however, if we assume

$$A(x) N(x) + \frac{\partial}{\partial x} [B(x) N(x)] = \text{const} \quad (11)$$

we obtain a stationary state which represents an open system where interaction among particles takes place. Equation 10 is no longer valid, and in this case we expect a family of solutions where equilibrium solution is a particular case of the stationary solution with the constant in eq 11 is zero. There are subtle differences in the two cases which have been discussed at length in ref 7. Here we are interested in the time dependent solution for a closed system, i.e., the one that approaches asymptotically to the equilibrium solution. From now on we will restrict our attention to a closed system where the asymptotic state is an equilibrium state and use eq 9 to determine  $N(x)$ . In general the coefficients  $A$  and  $B$  depend on the cluster size because the fluxes go down as the droplet grows due to the reduction in the difference of chemical potential between the droplet interiors and exteriors thereby lowering the effective diffusion transport. In this study we make a simplifying assumption that  $A/B$  is a slowly varying function of  $x$  (this is a reasonable assumption, as the validity of Fokker-Planck equation requires small increments for all  $x$ ). The above assumption is made with the possibility of achieving an analytical solution and with the hope that a good agreement between theory and experiment could eventually justify this assumption. Now eq 9 can be solved for  $N$ , giving

$$N(x) = n^{\text{eq}}(x_c) \exp[-(A/B)(x - x_c)] \quad (12)$$

where we have introduced the critical population  $x_c$  (corresponding to the population of droplet of critical radius) as the lower limit. This is justified because the droplets with radius smaller than the critical radius disappear due to Ostwald ripening.<sup>11</sup> We now proceed to solve the nonseparable part of the solution and assume

$$\Phi(x,t) = f(x + x_0(t), t) \quad (13)$$

where  $x_0(t)$  represent the average population of the

particles in a droplet or cluster. By writing  $\Phi(x,t)$  in this form, we are able to study the distribution about the mean value. Since the experiments indicate that the average value is a function of time, an explicit dependence on time is an obvious choice. Substituting eq 13 into eq 10, we get

$$\frac{\partial f}{\partial t} = B \frac{\partial^2 f}{\partial x^2} - A \frac{\partial f}{\partial x} - \frac{\partial x_0}{\partial t} \frac{\partial f}{\partial x} \quad (14)$$

In what follows, we will assume that both  $A$  and  $B$  are constants and define

$$\partial x_0 / \partial t = -A \quad (15)$$

Equation 14 reduces to a diffusion equation, which is

$$\frac{\partial f}{\partial t} = B \frac{\partial^2 f}{\partial x^2} \quad (16)$$

where  $B = (\alpha + \beta)/2$  and is not a diffusion coefficient normally used in the literature. Because of the nondimensional nature of our variable  $x$ ,  $B$  has the dimensions of  $\text{s}^{-1}$  instead of  $\text{cm}^2 \text{s}^{-1}$ . Later, when we compare theory with experiments, we will define and estimate as well the spatial diffusion coefficient in terms of  $\beta$ . Equation 15 can serve to determine the average population and can be easily solved to give

$$x_0(t) = x_c - At \quad (17)$$

where we have assumed that the population of droplet at  $t = 0$  is  $x_c$ , the population corresponding to the critical radius droplet. This is consistent with the above assumption that droplets with  $x < x_c$  will disappear. We note from eq 17 that for  $A > 0$ , the droplets will simply disappear and  $A < 0$  corresponds to the growth phase. For  $A = 0$  ( $\alpha = \beta$ ), the average population remains stationary at  $x = x_c$ . Equation 16 can be solved by standard techniques, and the solution is given by

$$f(x,t) = \int_{-\infty}^{\infty} f(\xi, t)|_{t=0} \frac{1}{\sqrt{4\pi Bt}} \exp\left[-\frac{(x - \xi)^2}{4Bt}\right] d\xi \quad (18)$$

To proceed further, we need initial conditions on the function  $f$  which is a mathematical function lacking physical meaning. However the function  $f$  is related to the cluster distribution  $n$ . From eq 7 and eq 13 and assuming that at  $t = 0$  we have a  $\delta$  function distribution for  $n$ , we can write

$$n(x,0) = n^{\text{eq}}(x) f(x + x_c, 0) = n^{\text{eq}}(x) \delta(x - x_c) \quad (19)$$

Replacing  $x$  by  $x - x_c$ , we have

$$f(x,0) = \delta(x - 2x_c) \quad (20)$$

Substituting eq 20 into eq 18, we get

$$f(x,t) = \frac{1}{\sqrt{4\pi Bt}} \exp\left[-\frac{(x - 2x_c)^2}{4Bt}\right] \quad (21)$$

Substituting eqs 13 and 21 into eq 7, we have

$$n(x,t) = \frac{n^{\text{eq}}(x_c)}{\sqrt{4\pi Bt}} \exp\left[-\frac{(x - x_0)^2}{4Bt}\right] \quad (22)$$

This shows that the size distribution of droplets or clusters formed under microgravity environment can be represented by a Gaussian with the mean and standard deviation given, respectively, by  $x_0(t)$  and  $\sqrt{2Bt}$ . Note that the parameters used in theory (population) and experiment (diameter) are not the same; a transformation is needed before we can make a direct comparison between the two.

Experiments show that the droplet distribution for specimens prepared under microgravity environment is more or less Gaussian. This is true even if the PDLC film is exposed to microgravity environment in the final stages of the growth phase. In other words microgravity or lack of gravitational forces can groom the droplet distribution so that the data fit a normal curve. Theoretically we have shown that when cluster-cluster aggregation, caused by gravitational forces, is neglected, the population distribution is Gaussian at all times with a time-dependent mean as also observed experimentally. Since the experimental data are given in terms of droplet diameter, we assume that

$$d = kx \quad (23)$$

where  $k$  has the dimension of length and is probably a function of time. Exact dynamical scaling is difficult to find from our experimental data because of the limitations imposed by the fixed drop time and combined growth under microgravity and terrestrial environment. However, to recover the classical results<sup>12,13</sup> ( $t^{1/3}$  dependence) where coarsening takes place via condensation and evaporation,  $k$  must be a decreasing function of time with  $t^{-2/3}$  dependence. In fact, from eq 17 during the later stages of the growth phase ( $\beta > \alpha$ ,  $d_0 > d_c$ ), we have

$$d_0(t) = -kAt = k\beta t \quad (24)$$

which shows that  $k \sim t^{-2/3}$  if we expect the classical result to be valid. As mentioned earlier the experimentally observed growth for mean droplet diameter is much faster than the  $t^{1/3}$  scaling, which we believe is due to coalescence processes. Substituting eq 23 into eq 22, we get

$$n(d,t) = \frac{kn^{\text{eq}}(d_c)}{\sqrt{2\pi\sigma}} \exp\left[-\frac{(d-d_0)^2}{2\sigma^2}\right] \quad (25)$$

where  $d_0$  is the mean droplet diameter and we have defined

$$\sigma^2 = 2k^2Bt \quad (26)$$

We now define an effective (because of combined growth) spatial diffusion coefficient by

$$D = k^2B \quad (27)$$

The plot of eq 25 is superimposed on the experimental data in Figure 4, which shows a reasonably good agreement for an estimated  $D = 3.78 \times 10^{-12} \text{ cm}^2 \text{ s}^{-1}$ .

(12) Landau, L. D.; Lifshitz, E. M. *Physical Kinetics*, Pergamon Press: New York, 1981; Chapter XII.

(13) Lifshitz, E. M.; Slyozov, V. V. *J. Phys. Chem. Solids* **1961**, *19*, 35.

While comparing Figures 3 and 4, we note that even if the droplets were permitted to grow initially under terrestrial conditions (4 s in this case) microgravity has a kind of grooming effect which produces more or less Gaussian distribution. One can easily argue that when coalescence of droplets is neglected, the growth is expected to be diffusion dominated. The aim here is not to show that the droplet growth is diffusional but develop a model which when combined with experimental results renders approximate estimate of the transport coefficient  $D$ .

## Conclusions

In conclusion we note that a microgravity environment not only produces more spherical droplets but also modifies the droplet distribution. We find that for combined growth, where initial growth is under terrestrial conditions and the final growth is under microgravity environment, the distribution is almost Gaussian as compared to the situation where the total growth takes place at  $1g$ . The coalescence processes at  $1g$  play an important role and produce non-Gaussian type of distribution. The important observation is that microgravity grooms the droplets in such a way that the distribution becomes Gaussian even if the microgravity exposure is in the final growth stage. The mean radius increases with time much faster than predicted by theory. We believe that this difference is due to coalescence processes during the cure time at  $1g$ . The growth at  $10^{-6}g$  is diffusion dominated with an estimated effective spatial diffusion coefficient of  $3.78 \times 10^{-12} \text{ cm}^2 \text{ s}^{-1}$  which seems reasonable for a polymer matrix environment. We find reasonable good agreement between theory and experiment.

**Acknowledgment.** This work was supported by the Natural Science and Engineering Research Council (NSERC) of Canada and the Canadian Space Agency (CSA). We are thankful to S. Gingras and M. Tabrizian for their technical assistance. J.M.J. is also gratefully to INRS for a postdoctoral fellowship.

## Appendix

The system of eq 1 when written explicitly for  $i = 1, 2, \dots, p$ , are

$$dn_1/dt = -\beta_1 n_1 + \alpha_2 n_2 \quad (\text{A}_1)$$

$$dn_2/dt = -(\alpha_2 + \beta_2)n_2 + \alpha_3 n_3 + \beta_1 n_1 \quad (\text{A}_2)$$

$$\frac{dn_{p-1}}{dt} = -(\alpha_{p-1} + \beta_{p-1})n_{p-1} + \alpha_p n_p + \beta_{p-2} n_{p-2} \quad (\text{A}_{p-1})$$

$$dn_p/dt = -\alpha_p n_p + \beta_{p-1} n_{p-1} \quad (\text{A}_p)$$

Note that  $\alpha_1 = \beta_0 = \alpha_{p+1} = \beta_p = 0$  by definition. Adding the above system, most of the terms cancel out and we

are left with

$$\frac{dn_1}{dt} + \sum_{j=2}^p \frac{dn_j}{dt} = 0 \quad (A_{p+1})$$

Substituting eq  $A_{p+1}$  into eq  $A_1$ , we get

$$\beta_1 n_1 = \alpha_2 n_2 + \sum_{j=2}^p \frac{dn_j}{dt} \quad (A_{p+2})$$

Equation  $A_{p+2}$  can be generalized to

$$\beta_k n_k = \alpha_{k+1} n_{k+1} + \frac{d}{dt} \left( \sum_{j=k+1}^p n_j \right) \quad (A_{p+3})$$

Now if we replace the discrete variable  $k$  by a continuous variable  $x$ , the sum over  $j$  is transformed into an integral with a lower limit  $x_{\min} = x + 1/2$  and an upper limit  $x_{\max} = p + 1/2$ . Each term in the sum is replaced by an area of a rectangle of unit width and the sum of the areas of the rectangles equals the area under the continuous

curve which is the integral of  $n(x)$ . Thus eq  $A_{p+3}$  can be written as

$$\beta(x) n(x, t) = \alpha(x+1) n(x+1, t) + \frac{d}{dt} \int_{x+1/2}^{x_{\max}} n(x, t) dx' \quad (p+4)$$

Differentiate eq  $A_{p+4}$  with respect to  $x$ , we get

$$\frac{d}{dt} n(x+1/2, t) = \frac{\partial}{\partial x} [\alpha(x+1) n(x+1, t) - \beta(x) n(x, t)] \quad (A_{p+5})$$

Change  $x + 1/2 \rightarrow x$  in eq  $A_{p+5}$ , we get

$$\frac{d}{dt} n(x, t) = \frac{\partial}{\partial x} [\alpha(x+1/2) n(x+1/2, t) - \beta(x-1/2) n(x-1/2, t)] \quad (A_{p+6})$$

Using Taylor's series expansion and assuming  $\alpha(x+1/2) \approx \alpha(x)$ , we get the Fokker-Planck equation.

CM950493K